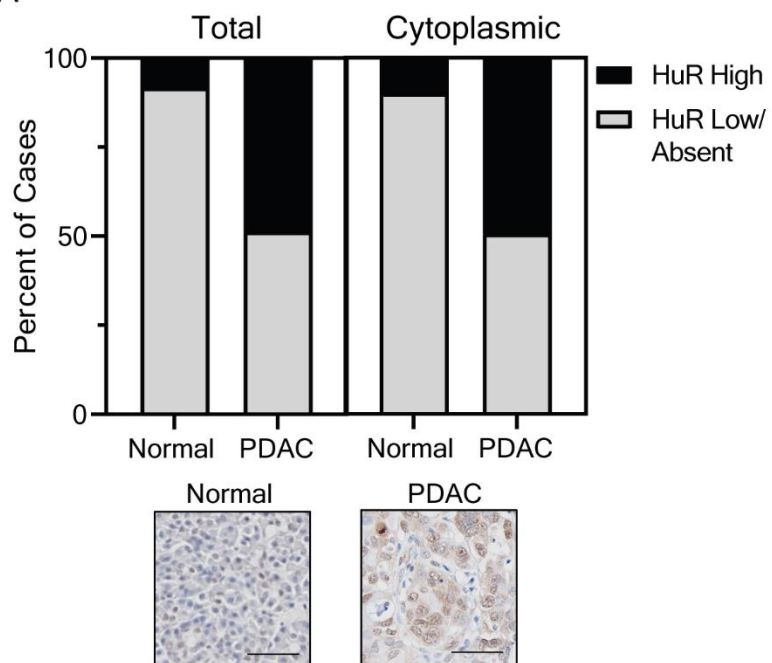
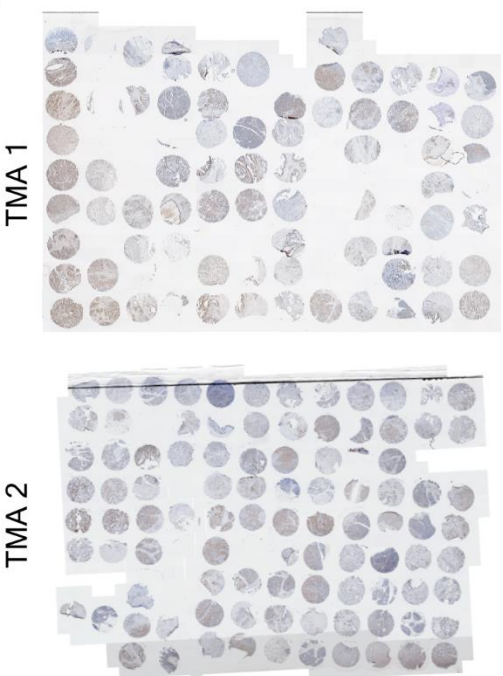


SUPPLEMENTAL FIGURES

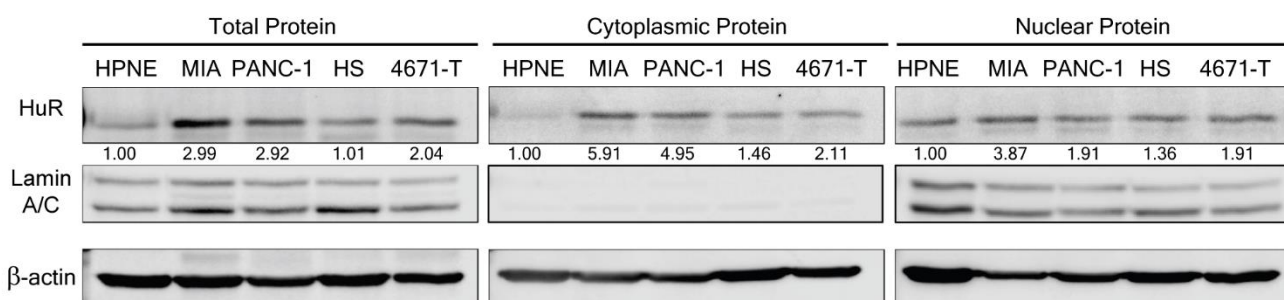
A



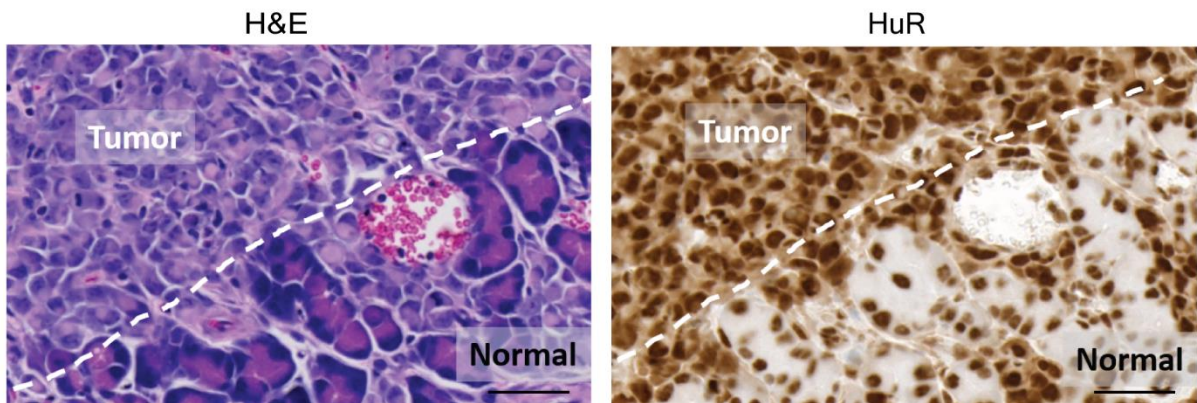
B



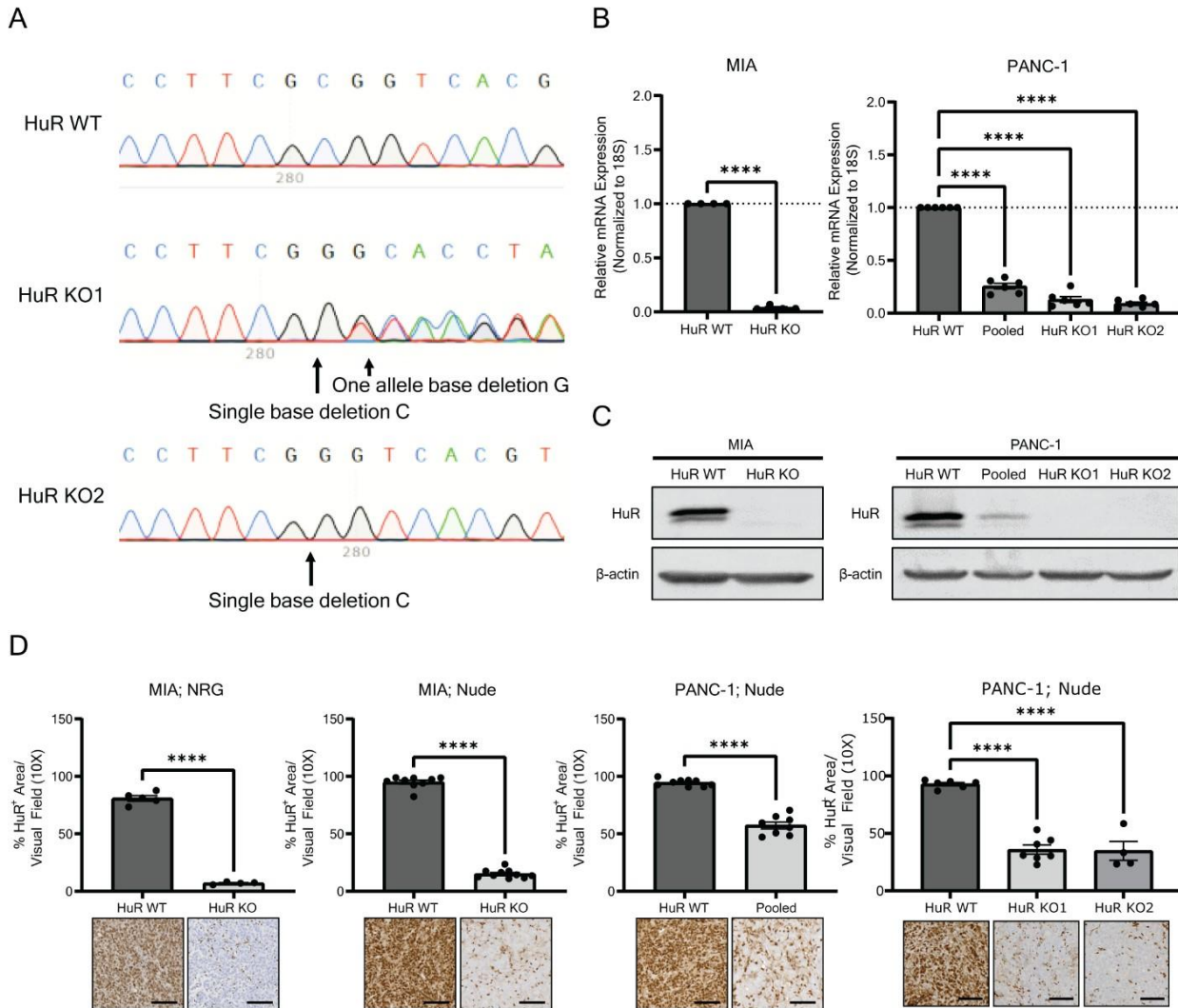
C



D

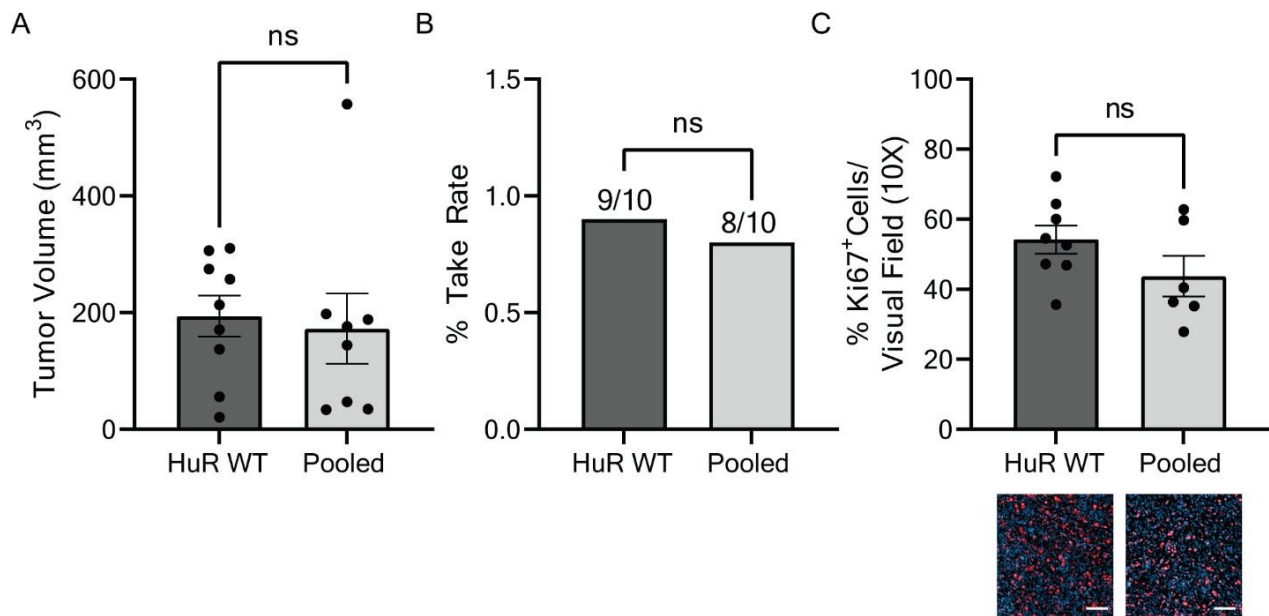


Supplemental Figure 1. HuR is highly expressed in pancreatic ductal adenocarcinoma. A) TMA created from patients at Oregon Health & Science University with normal pancreas (n=12) or PDAC tumors (n=77). TMA was stained for HuR and ductal cells were scored for total HuR expression by a pathologist. Cytoplasmic expression of HuR was scored by three authors and averaged for each core. Representative cores are found below the corresponding bar graph. B) Full panel of TMA cores quantified in A. C) Representative Western blot analysis of HuR from whole cell lysates, and cytoplasmic and nuclear fractions of an immortalized normal pancreatic ductal cell line (HPNE) and a panel of PDAC cells (MIA PaCa-2 (MIA), PANC-1, HS766t (HS), 4671-T-CRC (4671-T), n=3). Cell line 4671-T is a conditionally reprogrammed cell line generated from a primary human PDAC tumor at Oregon Health & Science University. Protein quantification indicated under each band was normalized to β -actin and relative to HPNE. D) Representative hematoxylin and eosin staining and HuR staining of MIA orthotopic mouse model showing tumor and normal pancreas tissue. Scale bars represent 50 μ m.

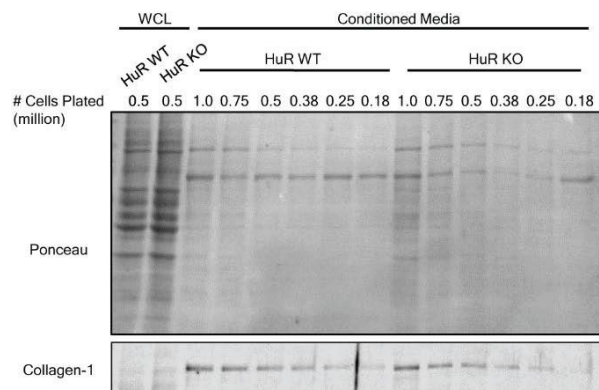
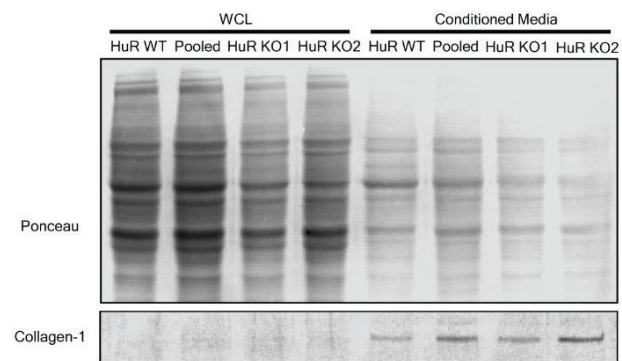


Supplemental Figure 2. Validation of CRISPR-mediated HuR KO cells and orthotopic tumors. A) Sanger sequencing of *ELAVL1* for PANC-1 HuR WT and two distinct HuR KO cells (HuR KO1 and HuR KO2), annotated for mutations. B) RT-qPCR analysis of HuR mRNA in MIA and PANC-1 cells. mRNA expression was determined using *18S* rRNA for normalization and relative to HuR WT expression. Statistical analysis was calculated using a Student's two-sample t-test for MIA and one-way ANOVA for PANC-1. C) Representative Western blot analysis of HuR protein expression in MIA and PANC-1 cells. β -actin was used as a loading control. D) Quantification of % HuR⁺ area/ visual field imaged at 10X. Each data point represents the average of at least 5 images/tumor stained for HuR. Representative images are found below the

corresponding bar graph. Tumors analyzed were from the orthotopic model of MIA cells injected in NRG mice, MIA cells injected in nude mice or PANC-1 cells injected in nude mice (also see **Supplemental Table 1**). Statistical analysis was calculated using a Student's two-sample t-test for all models except PANC-1; Nude orthotopic with clones, which was calculated using one-way ANOVA. Error bars represent standard error of the mean. ***p<0.0001. Scale bars represent 50 μm .

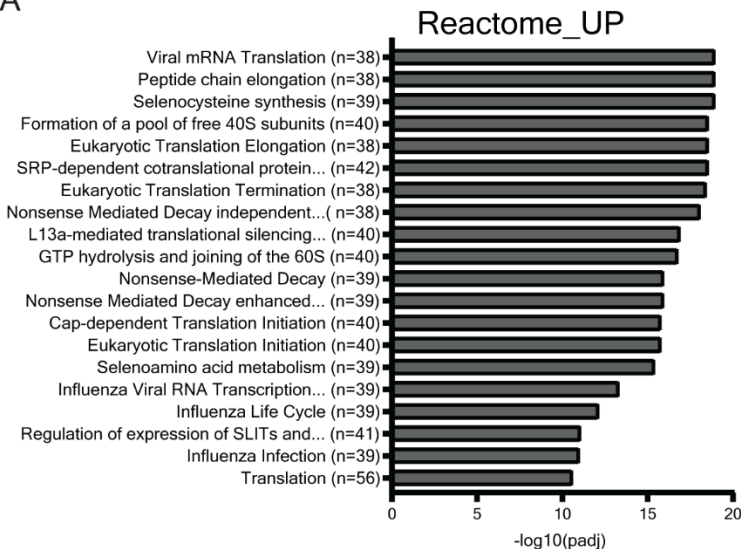


Supplemental Figure 3. Pooled tumors do not have altered tumor growth or proliferation in an orthotopic xenograft PDAC model. A) Tumor volumes of PANC-1 WT and Pooled tumors in nude mice. Each datapoint represents a separate tumor. B) Take rate of PANC-1 WT and Pooled tumors in nude mice. C) Quantification of % Ki67⁺ cells/ visual field imaged at 10X for PANC-1 WT and Pooled tumors in nude mice. Each datapoint represents the average of at least 5 images/tumor stained for Ki67. Representative images are found below the corresponding bar graph. Statistical analysis was calculated using a Student's two-sample t-test. Error bars represent standard error of the mean. ns, not significant. Scale bars represent 50 μm .

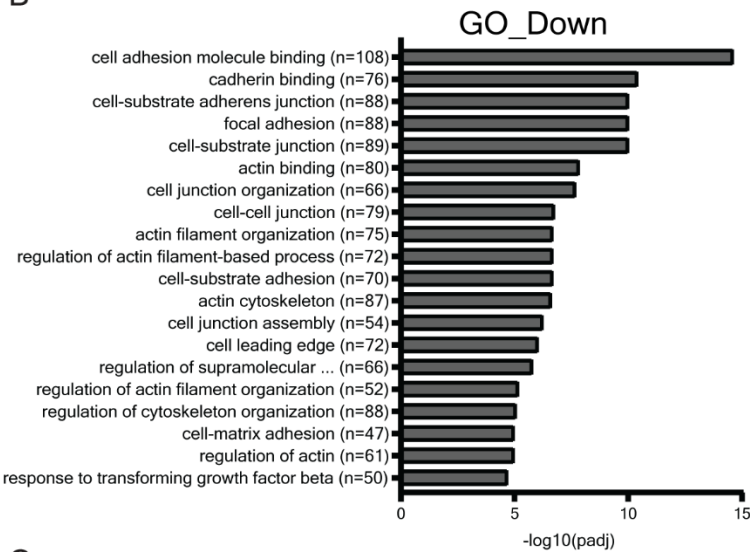
A**B****Supplemental Figure 4. Collagen secretion from PDAC cells is not impacted by HuR.**

Representative immunoblot analysis of collagen-1 from whole cell lysates (WCL) and conditioned media. A) MIA HuR WT and HuR KO cells were plated at the number of cells indicated above each lane. Ponceau stain was used as a loading control (n=3). B) 1E6 PANC-1 HuR WT, Pooled, HuR KO1, HuR KO2 cells were plated, and WCL and conditioned media were assessed for collagen-1. Ponceau stain was used as a loading control (n=3).

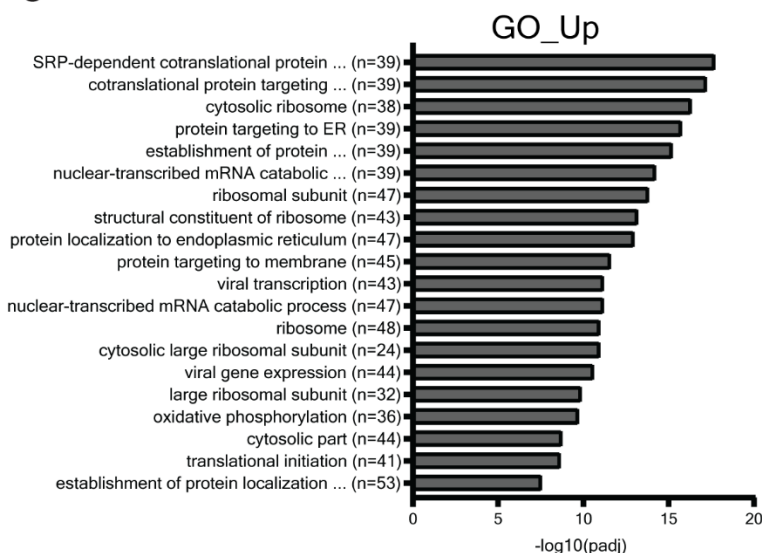
A



B

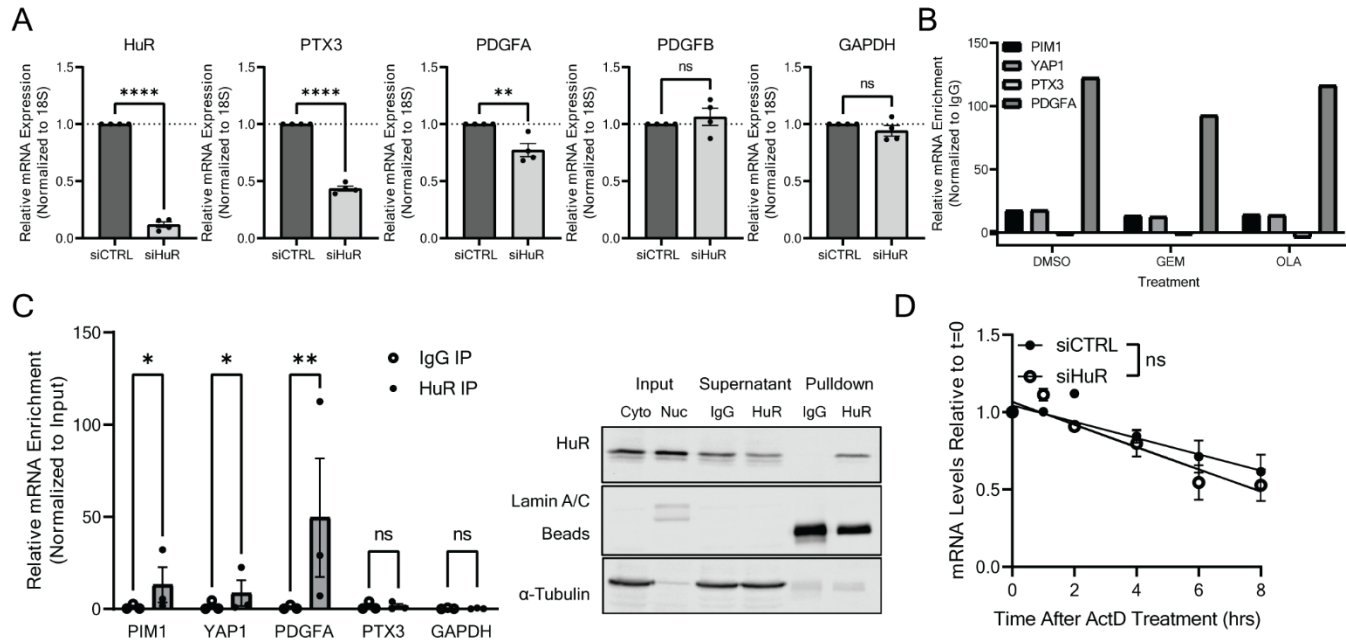


C

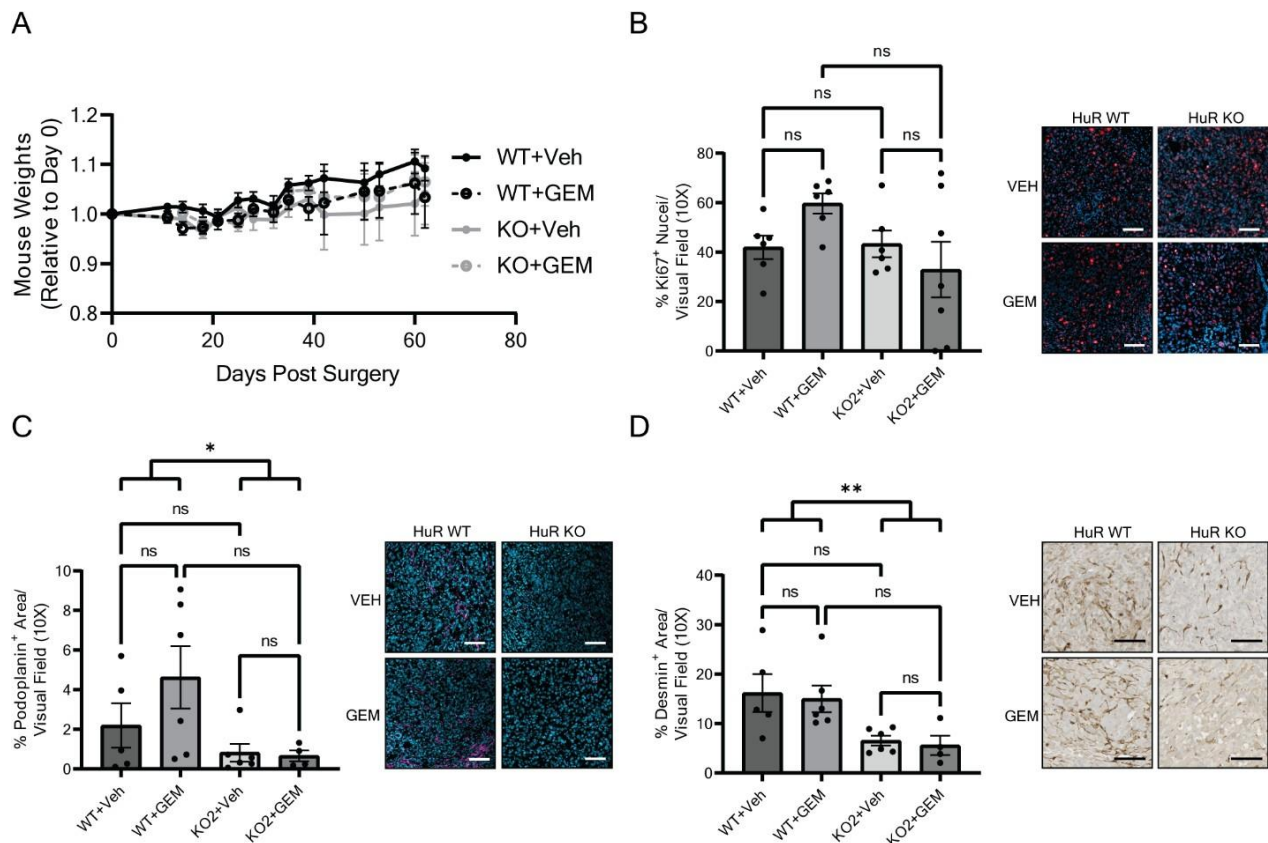


Supplemental Figure 5. Loss of HuR results in downregulation of cell adhesion pathways, and upregulation of transcription and translation processes. Analysis of RNA-sequencing of MIA HuR KO tumors compared to HuR

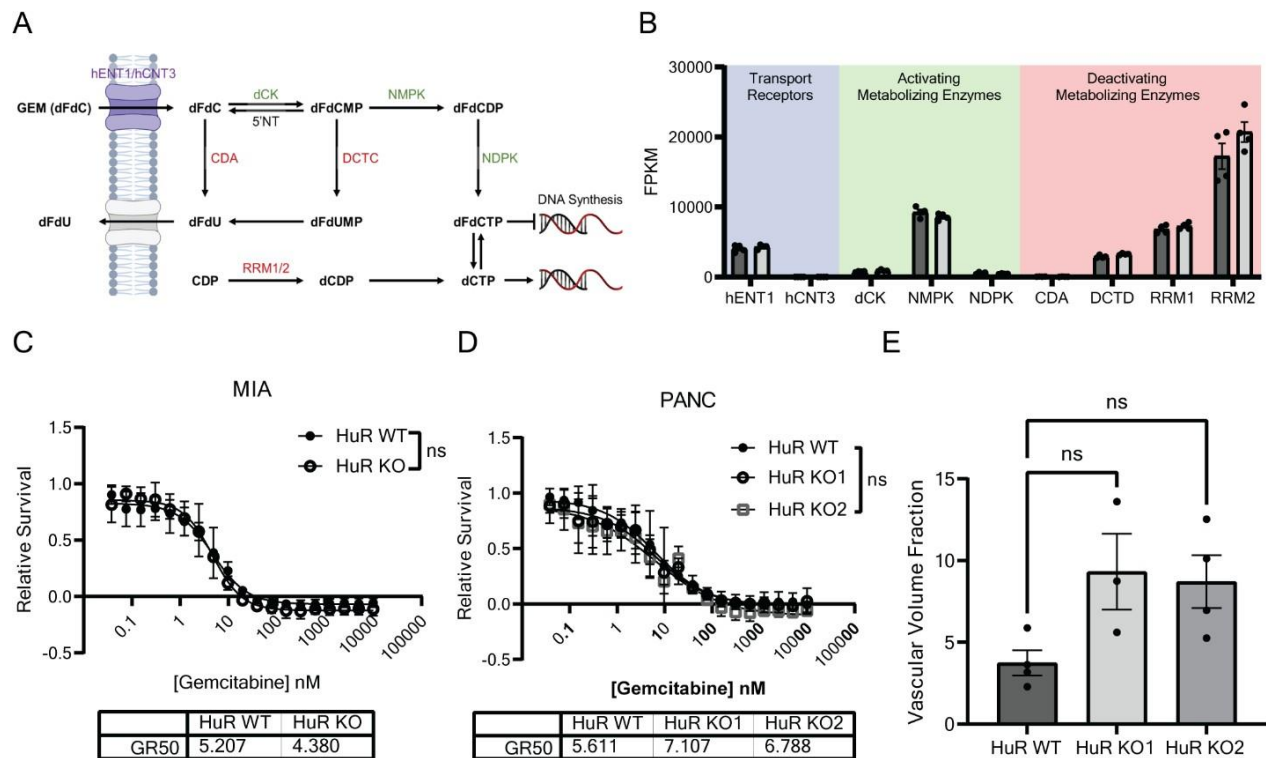
WT tumors. Top significantly A) upregulated Reactome pathways, B) downregulated GO pathways and C) upregulated GO pathways.



Supplemental Figure 6. HuR directly regulates PDGFA RNA. A) RT-qPCR analysis of mRNA in PANC-1 cells transfected with either siControl or siHuR. Statistical analysis was calculated using a Student's two-sample t-test. B) Analysis of *PTX3* and *PDGFA* mRNA pulldown with HuR in comparison to known HuR targets in published RIP-array (80) of MIA cells treated with either dimethyl sulfoxide (DMSO), gemcitabine (GEM), or olaparib (OLA). C) RIP analysis of *PTX3* and *PDGFA* mRNA pulldown with HuR in comparison to known HuR targets. Representative immunoblot validation of HuR pulldown in PANC-1 cells found to the right of the graph. D) PANC-1 cells were transfected with either siControl or siHuR and treated with actinomycin D. *PDGFA* mRNA levels were assessed at indicated time by RT-qPCR. Error bars represent standard error of the mean. ****p<0.0001, ***p<0.001, **p<0.01, *p<0.05, ns not significant.



Supplemental Figure 7. Loss of HuR maintains decreased stromal composition regardless of gemcitabine treatment. A) Mouse weights relative to day of surgical implantation from mice treated with either VEH or GEM. B-D) Quantification of B) % Ki67⁺ area, C) % podoplanin⁺ area, and D) % desmin⁺ area/ visual field imaged at 10X of tumors from **Figure 7A**. Each data point represents the average of at least 5 images/tumor. Statistical analysis was calculated using a one-way ANOVA. Error bars represent standard error of the mean. ***p<0.0001, **p<0.001, **p<0.01, *p<0.05, ns not significant. Scale bars represent 50 μ m.



Supplemental Figure 8. Loss of HuR does not impact GEM transporters, metabolizing enzymes or drug sensitivity *in vitro*, but may increase tumor blood volume *in vivo*. A) Diagram of gemcitabine metabolism adapted from Liang, C. *et al.* [3]. Figure created in BioRender. B) FPKM counts of receptors and metabolizing enzymes responsible for GEM toxicity assessed by RNA sequencing performed on MIA HuR WT and HuR KO cell lines. C-D) Relative cell survival of C) MIA and D) PANC-1 cells treated with GEM over 5 days. GR50s are noted under each graph. E) Vascular volume fraction of PANC-1 orthotopic tumors measured utilizing magnetic resonance imaging. Statistical analysis was calculated using a one-way ANOVA. Error bars represent standard error of the mean. ns not significant.

SUPPLEMENTAL TABLES

Supplemental Table 1: Demographic and clinicopathologic data for TMAs stained for HuR. IQR=

Interquartile Range. *Demographic data unavailable for n=1 patient. **Clinicopathologic data unavailable for n=61 patients.

Variable	N (%)
Age, years; median [IQR]*	66 [58-71]
Sex*	
Male	33 (43.4%)
Female	43 (56.6%)
Race/Ethnicity	
White	70 (90.9%)
Black	0 (0%)
Asian	2 (2.6%)
Hispanic	2 (2.6%)
Unknown/ Not reported	5 (6.5%)
Current/Prior Smoker**	9 (11.7%)
Tumor size, cm; median [IQR]**	2.5 [1.9-3.1]
Tumor Differentiation**	
Well	1 (6.2%)
Moderate	12 (75%)
Poor	3 (18.8%)
Node Positivity**	9 (56.3%)
Lymphovascular Invasion**	
Present	9 (56.3%)
Absent/Indeterminant	7 (43.8%)
Perineural Invasion**	
Present	11 (68.8%)
Absent/Indeterminant	5 (31.2%)

Supplemental Table 2: Various models used to assess loss of HuR and the resulting impacts on PDAC

TME. *Denotes in comparison to HuR WT tumors. **Results do not account for heterogeneous expression of HuR.

Cell Line	Mouse Strain	Immune Composition of Mouse Strain	HuR KO Cell Line	HuR Status	Tumor Growth*	Ki67 Staining*	Collagen Staining*	Podoplanin Staining*	αSMA Staining*	Desmin Staining*
MIA	NRG	Absent of mature B and T cells, NK cells; Defective DC cells and macrophages	KO	Absent	No change	No change	Decreased	Decreased	Decreased	Decreased
	Nude	Absent of mature T cells	KO	Absent	No change	No change	Decreased	Decreased	Decreased	Decreased
PANC-1	Nude	Absent of mature T cells	Pooled**	Heterogeneous	No change	No change	Decreased	Non-significant decrease	Non-significant decrease	Non-significant decrease
			KO1	Absent	No change	No change	Decreased	Decreased	Decreased	Non-significant decrease
			KO2	Absent	Non-significant increase	Non-significant decrease	Decreased	Decreased	Decreased	Non-significant decrease

Supplemental Table 3: Genes downregulated in cell-cell communication reactome pathway identified by RNA sequencing.

Sample	GeneRatio	BgRatio	pvalue	geneName	Count
HuR KO vs HuR WT_Cell Line	34/1688	115/8632	0.00625	SKAP2/FYN/CLDN11/CDH10/PIK3CB/LAMA3/COL17A1/NCK2/ACTN1/MPP5/FERMT2/ITGA6/WASL/PIK3CA/FLNC/AFDN/ITGB4/SDK1/CASK/RSU1/ITGB1/DST/F11R/FBLIM1/CLDN1/PRKCI/PTK2/LIMS1/CADM2/PARD6G/PTPN11/CDH5/CLDN4/CD47	34
HuR KO vs HuR WT_Tumors	37/942	111/8233	6.58E-10	CDH10/PIK3CB/COL17A1/NCK2/ACTN1/MPP5/FERMT2/PXN/WASL/NECTIN1/SPTBN1/PIK3CA/ITGB4/IQGAP1/SDK1/CASK/RSU1/ITGB1/DST/CDH12/F11R/FBLIM1/CLDN1/PRKCI/PTK2/CADM2/PLEC/PTPN11/CDH5/KIRREL1/KRT5/PARVB/CLDN4/CD47/LAMB3/FLNA/CTNNND1	37

Supplemental Table 4. Top 8 analytes showing significant impact on PDAC secretion with loss of HuR. Table includes fold change (FC) of secretion amounts from MIA HuR KO versus HuR WT cells, and pathways associated with the analyte.

Analyte	FC	Association
Pentraxin 3	0.07	ECM Organization, Inflammation
PDGF-AA	0.30	Mesenchymal cell infiltration, Stromal activation, Angiogenesis
VEGF	0.33	Angiogenesis
IL-24	0.33	Apoptosis, Wound-healing, Anti-inflammation
M-CSF	0.49	Macrophage proliferation
Angiogenin	0.49	Angiogenesis
CD14	2.72	Inflammation
GDF-15	7.54	Inflammation

Supplemental Table 5. Total impact of analyte secretion from PDAC cells with loss of HuR.

Table includes fold change (FC) of secretion amounts from MIA HuR KO versus HuR WT cells, and raw signal intensity values.

Analyte	WT				KO				Fold Change	
	Array 1		Array 2		Array 1		Array 2			
	Spot 1	Spot 2	Spot 1	Spot 2	Spot 1	Spot 2	Spot 1	Spot 2		
Adiponectin	1090	745	435	429	604	487	652	729	0.92	
Apolipoprotein A-I	281	282	304	327	255	290	158	263	0.81	
Angiogenin	8320	8650	9750	9430	4760	5120	4150	3860	0.49	
Angiopoietin-1	239	314	242	183	202	166	158	103	0.64	
Angiopoietin-2	677	619	455	433	475	501	464	425	0.85	
BAFF	596	330	269	256	188	300	185	213	0.61	
BDNF	619	525	354	384	387	286	374	366	0.75	
Complement Component C5/C5a	264	157	155	136	184	120	186	136	0.88	
CD14	564	648	455	424	1140	1180	1660	1720	2.72	
CD30	703	815	2080	2230	1850	2380	61	58	0.93	
CD40ligand	1050	1200	382	513	819	976	532	822	1.00	
Chitinase 3-like 1	260	215	249	161	98	155	115	182	0.62	
Complement Factor D	347	295	416	400	298	489	686	541	1.38	
C-Reactive Protein	377	301	367	281	317	164	255	261	0.75	
Cripto-1	241	224	161	158	142	165	168	196	0.86	
Cystatin C	1480	1230	1490	1520	893	928	1730	1970	0.97	
Dkk-1	16700	16700	9140	8980	18700	18500	14000	14400	1.27	
DPPIV	62.9	92	111	154	62.4	33.7	44	52	0.46	
EGF	265	137	184	72	60.2	66.8	212	171	0.78	
EMMPRIN	6550	6600	4940	4720	4110	5400	3220	3240	0.70	
ENA-78	16800	17600	17900	17300	12200	11500	9310	9350	0.61	
Endoglin	793	843	621	642	587	678	473	372	0.73	
Fas Ligand	199	224	246	163	169	174	270	149	0.92	
FGF basic	212	347	423	377	404	293	178	163	0.76	
FGF-7	79	68.7	185	181	126	159	124	73	0.94	
FGF-19	1170	1150	1250	1230	769	802	1200	1280	0.84	
Flt-3 Ligand	949	898	448	583	614	660	277	426	0.69	
G-CSF	617	505	324	300	288	274	240	257	0.61	
GDF-15	359	403	259	266	3500	3340	1390	1480	7.54	
GM-CSF	340	419	507	517	550	1680	486	495	1.80	
GRO α	11400	11700	11300	11400	9170	9320	8930	8320	0.78	
Growth Hormone	67.8	158	287	270	219	341	130	166	1.09	
HGF	254	268	246	118	139	122	152	151	0.64	
ICAM-1	429	474	283	400	262	313	225	310	0.70	
IFN- γ	502	439	341	463	255	207	400	337	0.69	
IGFBP-2	235	223	291	201	221	215	332	284	1.11	
IGFBP-3	239	126	146	162	129	129	132	241	0.94	
IL-1 α	513	643	46	493	418	388	282	405	0.71	
IL-1 β	209	262	189	173	135	150	164	208	0.79	
IL-1ra	163	148	165	182	56.6	108	95	171	0.65	
IL-2	326	339	161	283	169	207	265	297	0.85	
IL-3	137	137	296	268	111	178	191	201	0.81	
IL-4	281	231	479	351	336	433	223	205	0.89	
IL-5	53.8	68.3	157	59	110	82.5	63	62	0.94	
IL-6	490	523	453	742	382	354	300	690	0.78	
IL-8	22600	22300	Infinity	20500	17300	20100	16600	15600	0.80	
IL-10	334	215	404	358	159	132	330	247	0.66	
IL-11	489	475	392	357	312	254	348	365	0.75	
IL-12 p70	348	437	303	329	233	224	226	139	0.58	
IL-13	124	146	154	143	82.9	123	49	209	0.82	
IL-15	337	344	209	163	126	143	241	203	0.68	
IL-16	188	168	195	124	129	98.5	174	154	0.82	
IL-17A	1470	1490	996	944	898	888	1150	1220	0.85	
IL-18Bpa	136	223	231	256	409	457	267	393	1.80	
IL-19	193	216	261	421	175	259	197	195	0.76	

IL-22	309	313	359	379	259	183	315	263	0.75
IL-23	243	171	162	125	130	42.8	106	215	0.70
IL-24	1210	1460	985	1120	286	372	436	493	0.33
IL-27	268	271	201	214	142	147	101	127	0.54
IL-31	95.7	102	175	209	129	127	160	217	1.09
IL-32	154	288	144	122	170	187	201	114	0.95
IL-33	143	128	67	201	70.4	120	213	61	0.87
IL-34	299	360	264	252	206	110	191	191	0.59
IP-10	193	66.6	201	137	146	158	144	187	1.06
I-TAC	183	152	252	243	162	81.3	206	186	0.77
Kallikrein 3	565	593	515	531	268	358	362	389	0.62
Leptin	187	71.6	207	181	136	157	183	189	1.03
LIF	172	156	272	293	383	310	226	195	1.25
Lipocalin-2	300	279	297	326	249	207	277	262	0.83
MCP-1	526	507	292	393	236	206	357	316	0.65
MCP-3	153	209	144	186	44	108	136	100	0.56
M-CSF	1510	1730	1670	1690	852	838	772	763	0.49
MIF	5140	5360	5610	5490	4830	4760	5240	5090	0.92
MIG	201	168	255	169	119	146	193	251	0.89
MIP-1 α 'MIP-1fl	144	118	83	92	86	125	78	110	0.91
MIP-3a	161	135	171	146	139	93.8	167	136	0.87
MIP-3fl	174	233	112	101	85	136	161	176	0.90
MMP-9	197	364	393	301	565	719	632	697	2.08
Myeloperoxidase	141	151	206	321	128	100	145	82	0.56
Osteopontin	904	1060	926	880	669	397	896	1300	0.87
PDGF-AA	5180	5310	5210	5460	1900	1890	1280	1250	0.30
PDGF-AB/BB	366	371	248	222	236	258	215	213	0.76
Pentraxin 3	5670	5260	5680	5670	485	441	389	354	0.07
PF4	171	254	207	197	98	128	235	100	0.68
RAGE	252	278	323	427	178	201	226	188	0.62
RANTES	11700	12100	12100	11700	10700	10800	6890	7150	0.75
RBP-4	339	313	458	408	219	163	388	380	0.76
Relaxin-2	373	366	233	204	174	-20.4	298	203	0.56
Resistin	389	443	315	194	136	119	409	210	0.65
SDF-1 α	528	576	476	466	291	322	483	516	0.79
Serpin E1	16200	16300	16800	7850	13500	13600	14600	15100	0.99
SHBG	264	209	454	332	403	362	520	418	1.35
ST2	193	186	209	86	132	112	128	122	0.73
TARC	190	184	93	167	120	124	154	140	0.85
TFF3	323	303	308	389	88	63.7	125	112	0.29
TfR	1570	1500	1230	1220	1180	1530	1190	1210	0.93
TGF- α	152	105	234	98	124	86.3	70	69	0.59
Thrombospondin-1	596	740	650	553	356	331	319	334	0.53
TNF- α	177	140	218	153	123	151	129	222	0.91
uPAR	979	862	503	643	896	929	629	855	1.11
VEGF	7280	7630	6360	6310	3460	2680	1480	1470	0.33
Vitamin D BP	389	415	409	344	292	172	327	311	0.71
CD31	221	219	163	205	-44.1	-1.53	148	149	0.31
TIM-3	244	212	183	176	114	125	70	207	0.63
VCAM-1	367	441	333	324	198	-26	392	247	0.55